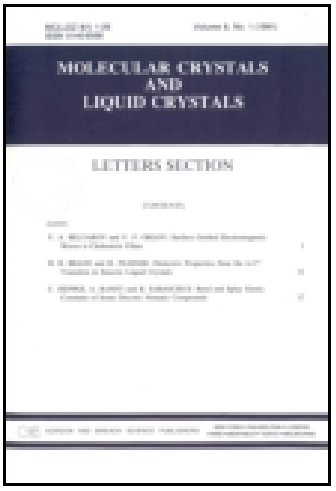

Molecular Crystals and Liquid Crystals
Publication details, including instructions for authors and subscription information:
http://www.tandfonline.com/loi/gmcl20

Viewing Angle and Imaging Polarization Analysis of Liquid Crystal Displays and Their Components

Thierry Leroux[a] & Pierre Boher[a]
[a] ELDIM, Hérouville St. Clair, France
Published online: 30 Sep 2014.

To cite this article: Thierry Leroux & Pierre Boher (2014) Viewing Angle and Imaging Polarization Analysis of Liquid Crystal Displays and Their Components, Molecular Crystals and Liquid Crystals, 594:1, 122-139, DOI: 10.1080/15421406.2014.917500

To link to this article: http://dx.doi.org/10.1080/15421406.2014.917500

Mol. Cryst. and Liq. Cryst, Vol. 594: pp. 122–139, 2014

ISSN: 1542-1406 print/1563-5287 online
DOI: 10.1080/15421406.2014.917500

Taylor & Francis
Taylor & Francis Group

Viewing Angle and Imaging Polarization Analysis of Liquid Crystal Displays and Their Components

THIERRY LEROUX* AND PIERRE BOHER

ELDIM, Hérouville St. Clair, France

Optical characterization of all types of displays is mandatory to quantify the different imperfections and compare the different technologies. Standard characterization is focused on luminance and color measurements of the light emitted by the displays. Viewing angle measurements devoted to the angular characterization and homogeneity measurements are the most frequently used. In the present paper we demonstrate that the same type of measurements extended to the polarization analysis of the light emitted by the display can be a powerful tool in order to understand the origin of many imperfections. The present paper is composed of two main parts: first the different measurement tools for viewing angle and imaging characterization are presented and the method used to analyze the polarization state of the light is explained. The second part gives details on some examples of applications for the characterization of display components (brightness enhancement film, backlight), the measurement of the crystal cell rotation inside a standard LCD display, and the characterization of a passive 3D TV.

Keywords 3D displays; polarization; viewing angle; imaging

Introduction

Liquid crystal (LC) technology is presently used inside almost all types of commercial applications involving displays. For auto-stereoscopic 3D displays it is even used to build LC lenses to control the angular emission. Liquid crystal cell is essentially a polarization state modulator and the polarization state of the light is a tool of choice to measure precisely the performances of such devices. Moreover, many components inside the displays are changing the polarization state of the light in a deliberate way (polarizer, LC cell, phase shift film . . .) or in an unintended way (brightness enhancement films, light guides, mirrors . . .). To understand the internal behavior of most of the displays, the polarization behavior of all the components of a display must be taken into account. In addition, in some cases the polarization state of the light emitted by the display can be used directly to provide the stereoscopic effect to the observer. It is the case for the passive glasses 3D displays which are presently the most common commercial solution for 3D TV. In this case, polarization analysis of the light seems the most natural solution to evaluate the quality of the stereoscopy.

Nevertheless this type of measurement is not very common presently. Most of the optical characterizations are presently focused on luminance and color measurements probably because they are directly sensitive to the human eye on the contrary of the polarization state.

*Address correspondence to Thierry Leroux, ELDIM, 1185 rue d′Epron, 14200 Hérouville St. Clair, France. E-mail: tleroux@eldim.fr

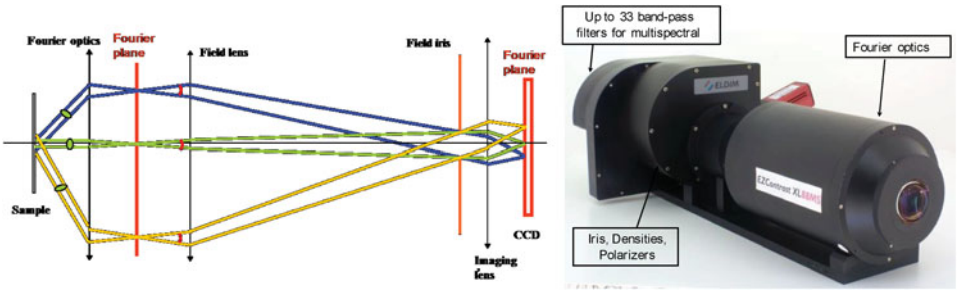

Figure 1. Schematic diagram of the viewing angle measurement system and photograph of EZContrastMS system.

The basis of polarimetry has been clearly expressed in the 1800's when Biot developed the first documented polarimeter [1]. Polarimetry has been intensively used in biomedical physics as for example recently for skin cancer detection [2], but the characterization of display has been quasi unexplored if we except the work made by our company. The present paper will try to make a synthesis of different ELDIM contributions made these last years. We have introduced the ability to measure spectral radiance and polarization state of the light in our Fourier optics viewing angle instruments in 2008 [3, 4]. We have shown that this type of measurement is especially helpful for LCD characterization [5, 6] and in particular for passive glass 3D displays [7, 8]. Polarization imaging has also been introduced recently by ELDIM for the characterization of displays and their components [9, 15]. In the present paper, after a presentation of the different measurement instruments and their capacities, we have selected some experimental examples to enlight the interest of measuring the polarization state in addition to standard light measurements. A first example concerns some brightness enhancement films (BEF) used routinely inside backlight system. Another example shows how to measure directly the rotation of the crystal cell inside a LCD. The last one is dedicated to the characterization of a passive glass 3D TV.

Experimental Details

Viewing Angle Measurements

ELDIM was founded in 1991 to promote an innovative display measurement instrument based on Fourier optics. A specific optic is designed in order to convert angular field map into a planar one allowing very rapid measurements of the full viewing cone (cf. Fig. 1a). This fast viewing angle measurement was first publicly introduced at Eurodisplay 1993 in Strasbourg [16]. Each light beam emitted from the sample surface with an angle θ with regards to the normal of the surface is focused on the Fourier plane at the same azimuth and at a position $x = F \tan(\theta)$. The angular emission of the sample is then measured simply and quickly without any mechanical movement. In practice, the Fourier optics is an achromatic combination of different lenses (6 to 9) that collects quasi all the light coming from the display and focus each angle on an intermediate Fourier plane (cf. Fig. 1a). A field lens and an imaging lens are then used to re-image the first Fourier plane on the CCD sensor. The design used by ELDIM includes a field iris before the sensor which is

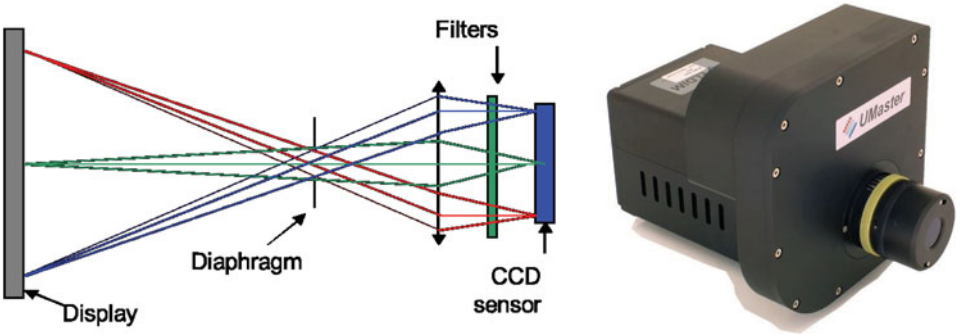

Figure 2. Schematic diagram of the imaging measurement system and photograph of UMaster system.

complex conjugate of the display surface and allows adjusting the measurement spot size independently to the angular aperture. As a consequence, the measurement spot size varies with the angle. This "cosine compensation" is mandatory to get good collection efficiency even for large incidence angles. The size of the measuring spot is easily adapted by the iris diameter. The optical path is quasi telecentric on the sensor side and so color or band pass filters can be positioned just before the sensor in order to perform color or spectral measurements. The ELDIM EZContrastMS system reported in Fig. 1b allows spectral measurement in all the visible range with a resolution of 10 nm (31 band pass filters from 400 to 700 nm).

Imaging Measurements

Imaging colorimeters are all based on CCD sensors and generally color filters. The difference between the systems lays in the accuracy, the signal over noise ratio, the spatial resolution and the quality of the imaging optics. ELDIM UMaster system (cf. Fig. 2b) is based on a Peltier cooled CCD sensor with 16 true bits analog digital converter. Five color filters dedicated to each CCD sensor are mounted on a motorized color wheel. The imaging optics is telecentric on the sensor side (cf. Fig. 2a), which ensures the same incidence for all the rays crossing the filters and so the same spectral response. In addition the flux collection is quasi-independent of the object distance while conventional optic can suffer from up to 20% reduction at short distance [9]. Different objectives with various angular apertures are available ($\pm 8^\circ$, $\pm 16^\circ$ and $\pm 30^\circ$). Another important parameter is the size of the entrance iris of the optical system. In the system of Fig. 2a, it can be adjusted to a value comparable to the human iris diameter without problem. With a conventional imaging objective the size of the first lens defines this parameter and is generally much larger than the human iris.

Polarization Analysis of the Light

For an arbitrary polarization state, the polarized component can be defined by its elliptical coefficients (ellipticity ε and orientation α) (cf. Fig. 3a), and the unpolarized component by the degree of polarization ρ given by the ratio of the intensity due to polarized component

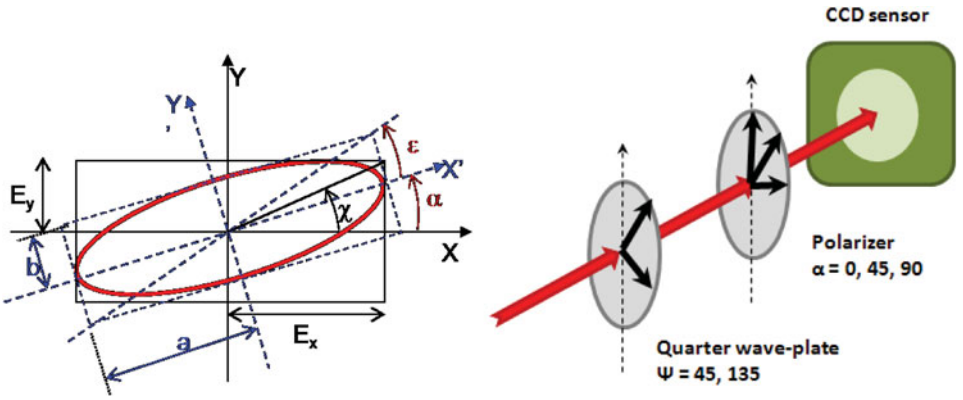

Figure 3. Definition of the ellipticity and additional optical elements used for polarization measurements.

over the total light intensity. We can also use the four Stokes parameters which are related to the previous one by:

$$S = \begin{bmatrix} I \\ Q \\ U \\ V \end{bmatrix} = I. \begin{bmatrix} 1 \\ \rho.\cos 2\varepsilon.\ \cos 2\alpha \\ \rho.\cos 2\varepsilon.\ \sin 2\alpha \\ \rho.\sin 2\varepsilon \end{bmatrix}$$

Measuring all four Stokes parameters requires absolute intensity measurements. However, the polarization state is completely determined by the three ratios Q/I, U/I, V/I, which we shall call the relative Stokes parameters. They then have possible values between -1 and $+1$. Many methods exist to measure the Stokes parameters [17, 18]. We have selected a simple one that consists in introducing additional polarization elements in the optical path (polarizers and wave plates) and making different images for different configurations. The advantage is the simplicity, the robustness and the stability but the measurement time is multiplied by seven compared to standard parameters.

The Stokes vectors of an incoming light can be obtained using the combination of a polarizer and a wave-plate as shown in Fig. 3b. Three measurements with a single polarizer at three orientations are sufficient to extract Q and U.

$$\frac{M(\theta) - M(\theta + \pi/2)}{M(\theta) + M(\theta + \pi/2)} = \frac{Q}{I} \text{ and } \frac{2M(\theta + \pi/4) - M(\theta) - M(\theta + \pi/2)}{M(\theta) + M(\theta + \pi/2)} = \frac{U}{I}$$

Three additional measurements combining polarizer and wave-plate of phase shift φ are necessary to get information on the degree of polarization.

$$\frac{M(\theta, \beta + \pi/2) - M(\theta, \beta)}{M(\theta, \beta) + M(\theta + \pi/2, \beta)} = \frac{V}{I} \sin\varphi \text{ and } \frac{M(\theta, \beta + \pi/2) - M(\theta\ + \pi/2, \beta)}{M(\theta, \beta) + M(\theta + \pi/2, \beta)} = \frac{Q}{I} \cos\varphi$$

In practice the system measures seven configurations and deduces directly the Stokes vectors and polarization coefficients for all the pixels of the CCD detector. The polarization elements are positioned near the diaphragm inside the two optical setups for viewing angle (cf. Fig. 1a) and imaging (cf. Fig. 2a). For viewing angle, the possible parasitic polarization introduced by the first part of the optics (Fourier and field lenses) cannot be corrected

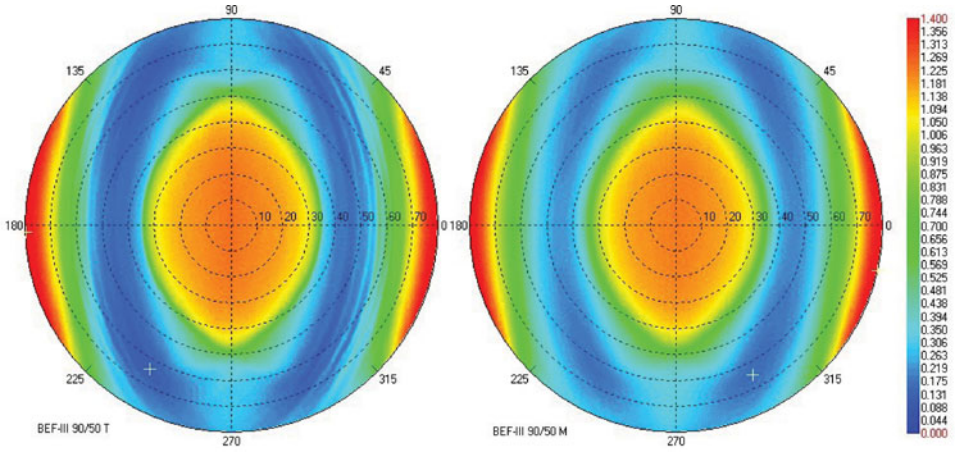

Figure 4. Angular transmittance measured at 538nm in full diffused illumination on a BEF-III 90/50-T film (left) and a BEF-III 90/50-M film (right).

easily. We have minimized this effect in the optical design (incident angles on the different surfaces of the lenses below 15°) and in the manufacturing. Parasitic polarization is below ±1% for incident angles below 50° and less than ±3% below 80°.

Experimental Results

Bright Enhancement Films

BEF films have generally a prismatic structure that use refraction and reflection to increase the efficiency of the backlight. The light is refracted within the viewing cone toward the viewer and reflected back outside it. The light can be recycled until it exits at the proper angle. In the following we have measured a Vikuiti BEF III film that includes a random prism pattern BEF-III 90/50-T and an additional optional matte film BEF-III 90/50-M. The polarization behavior of such a film is important since only one polarization of the backlight is used by standard LCD structures.

One example of transmittance measurement obtained using a quasi Lambertian light source is reported in Fig. 4. The transmittance of ∼120% up to 25° of incidence corresponds to the expected enhancement around normal incidence. Very small transmittance differences for films with or without matte layer below the prismatic structure can be noticed. In the region of limited transmittance above ∼25° sharp modulations can be noticed but their amplitude is quite small. The effect of the matte layer can be much more put in evidence when comparing the polarization variations reported in Fig. 5. The measurements are made with the same pseudo Lambertian source that is quasi not polarized. After crossing the films the polarization state of the light is much more complex. Strong polarization modulations can be noticed at very precise angles for the film without matte layer (cf. Fig. 5a). The matte layer reduces these modulations producing a light that is quasi unpolarized (cf. Fig. 5b).

To illustrate the impact of such BEF films on the overall characteristics of the backlight itself, polarization imaging can be performed directly using the system discussed previously. One example of such measurement is reported in Fig. 6. If the intensity of the light

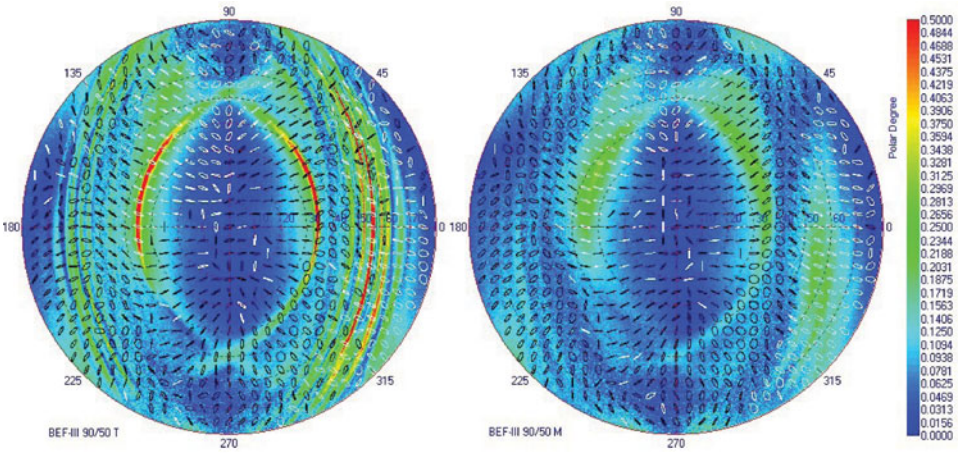

Figure 5. Polarization state measured at 538 nm in full diffused unpolarized illumination on a BEF-III 90/50-T film (left) and a BEF-III 90/50-M film (right); color scale refers to the polarization degree; ellipses colors refer to left and right side circularities.

(First Stokes vector component on Fig. 6a) does not show any specific feature, a pseudo periodic structure is detected on the polarization state across its surface (cf. Fig. 4b). This behavior has certainly an important impact on the homogeneity of the LCD build with this backlight.

LCD Display Without Top Polarizer

Polarization analysis of the light emitted by LCDs is also very informative on the efficiency of the liquid crystal cell as polarization modulator. We have already shown that unpolarized light detected in OFF state is directly related to the quality of the black level of the display [3]. Another way to follow in details the crystal cell switching is to remove the top polarizer of the LCD and to measure the polarization state versus grey level. One example is reported in Fig. 7. We see directly that the OFF state is characterized by quasi linear polarized light in particular near normal incidence. The liquid crystal cell rotation acts as a wave plate and the light becomes nearly circularly polarized for ON state. The polarization degree is also

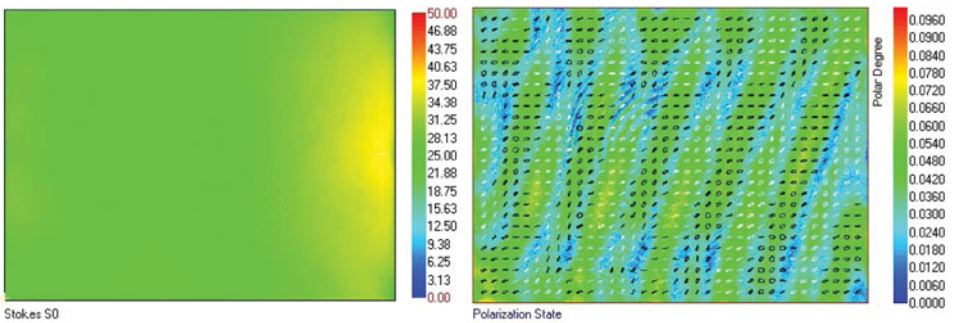

Figure 6. First Stokes vector component and polarization state measured at 550 nm on a LCD backlight with BEF film.

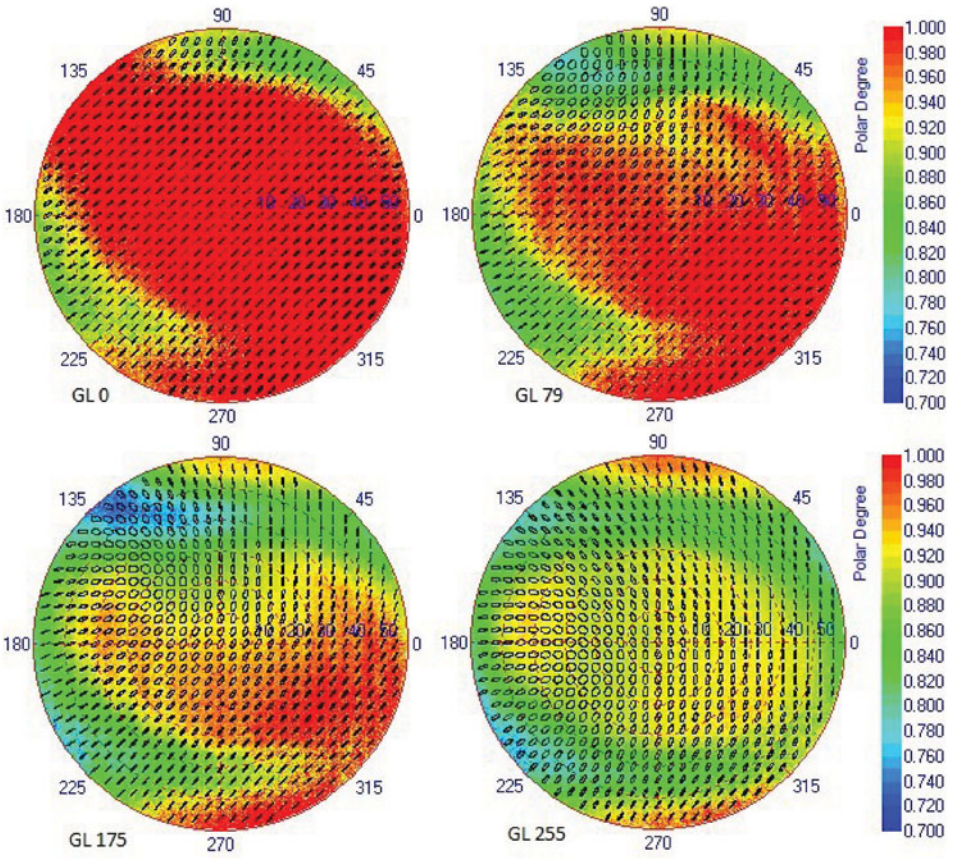

Figure 7. Polarization analysis of a LCD display without top polarizer: the measurement is made at 549 nm for four different grey levels (0, 79, 175 and 255).

slightly affected by the crystal cell rotation: it is nearly 1 for OFF state and decrease down to 0.85 for ON state.

The polarization rotation depends on the incidence and azimuth angles and drives the viewing angle of the display. As shown in Fig. 7, the polarization state of ON state is far to be ideal. In particular the light is not perfectly circular and strongly depends on the angle. To emphasize this point, we have reported the data measured along the 45° azimuth versus incidence angle and grey level (cf. Fig. 8). The wavelength is fixed at 549nm as for Fig. 7. We see that the maximum of ellipticity is not for normal incidence and does not reach 45°. The degradation of polarization degree at high angles drives the angle of view of the display. All these data can be used to evaluate the best top surface polarizer. One easy way to read the polarization data is to use the Poincare sphere as shown in Fig. 8. The evolution of the S1 and S2 Stokes vector is characteristic of the polarization rotation of the crystal cell and the influence of the incidence angle is particularly clear. The influence of the LC can be decomposed in an equivalent optical retardation and one rotation [19]. These two parameters can be easily driven from the present data. The rotation is in particular strongly dependent on the angle. The retardation is exactly at 45° only for +50° incidence in this case. The rotation and the orientation of a combine wave plate and polarizer to complete the LCD in the most efficient conditions can be derived. The efficient of the display must be

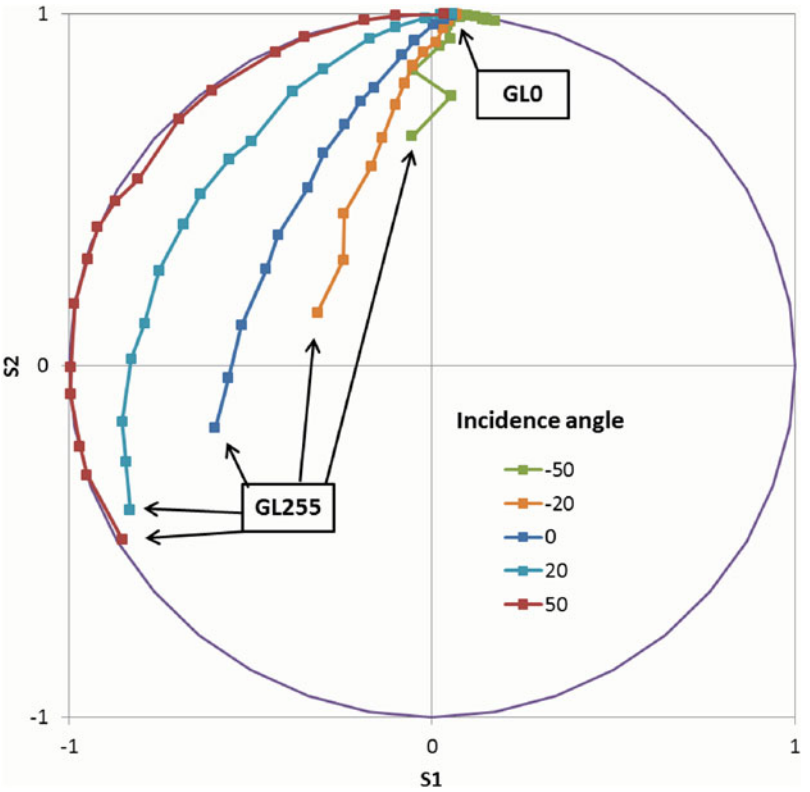

Figure 8. Stokes vector behavior of a LCD display without top polarizer versus grey level for five incidence angles along 45° azimuth: the wavelength is fixed to 549 nm.

also maximized for all the visible range. Using the same kind of measurements for different wavelengths such evaluation can be easily done.

Passive Glass 3D Displays

Stereoscopic displays require users to wear glasses to ensure that left and right views are seen by the correct eye. In the display under investigation, a standard LCD panel is completed with an additional phase difference film that convert linearly polarized light in right and left circular polarized light depending on the pixel line (cf. Fig. 9a). The images for left and right eyes are displayed simultaneously on even and uneven panel lines with half vertical resolution. The discrimination between the two images is performed with glasses that include a retarder and a polarizer with different orientation for left and right eyes.

Viewing Angle Measurements

Multispectral viewing angle polarization measurements have been performed on a passive glass LG 42LW650s TV for right view ON and left view OFF and the opposite. On the viewing angle pattern measured at 533 nm (cf. Fig. 10), we notice a vertical modulation of the ellipticity and the polarization degree. The ellipticity is around 45° (circular polarization)

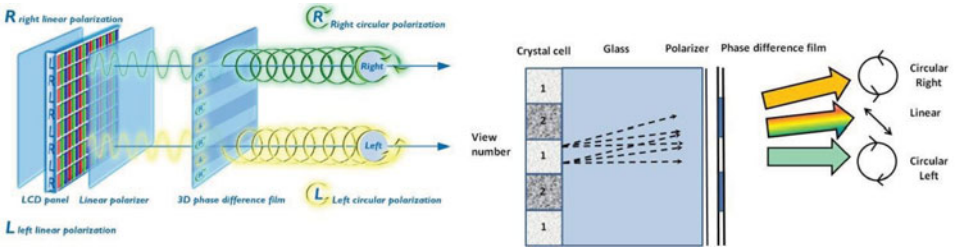

Figure 9. Principle of passive glass 3D displays and intermixing effect along vertical direction when phase difference film is glue on the glass top surface.

for a limited range of angles along the horizontal direction. In these regions, the polarization degree is near 95% but is reduced drastically outside. To work ideally the display must show a perfectly circular polarization with a polarization degree of 100%. Otherwise, the light is not completely stopped by the glass filter of the other eye and the contrast is reduced. The vertical modulation is due to a perspective effect induced by the location of the retarder film with regards to the crystal cell. In this display, the film is located on the display top surface (cf. Fig. 9b). The thickness of the top glass modulates the polarization of one view along vertical from right circular state to left circular state. So only one restricted part of the space in front the display is available for correct 3D perception. It is possible to suppress this modulation by including the phase difference film directly inside the display cell structure.

The spectral dependence of the polarization components is particularly interesting to analyze. In particular, the polarization degree does not exceed ∼90% even at the best angles and the best wavelength (cf. Fig. 11). This is especially important since the unpolarized component cannot be stopped by the circular polarizers included in the glasses and the 3D contrast will be therefore strongly reduced. Another source of imperfection is the ellipticity which never reaches its best value (circular state at ±45°). It is in fact also extremely

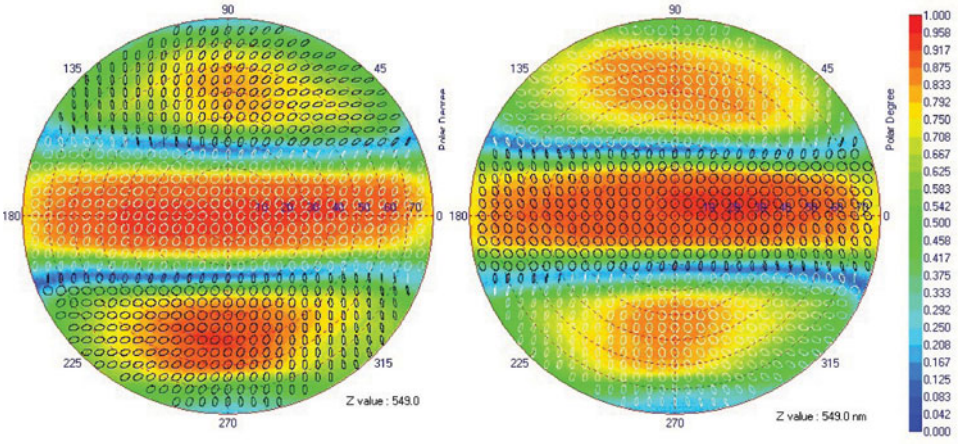

Figure 10. Polarization state measured at 549 nm for left and right eye views: the polarization ellipse and the degree of polarization are reported simultaneously; the black and white colors of the ellipses are for left and right circularity.

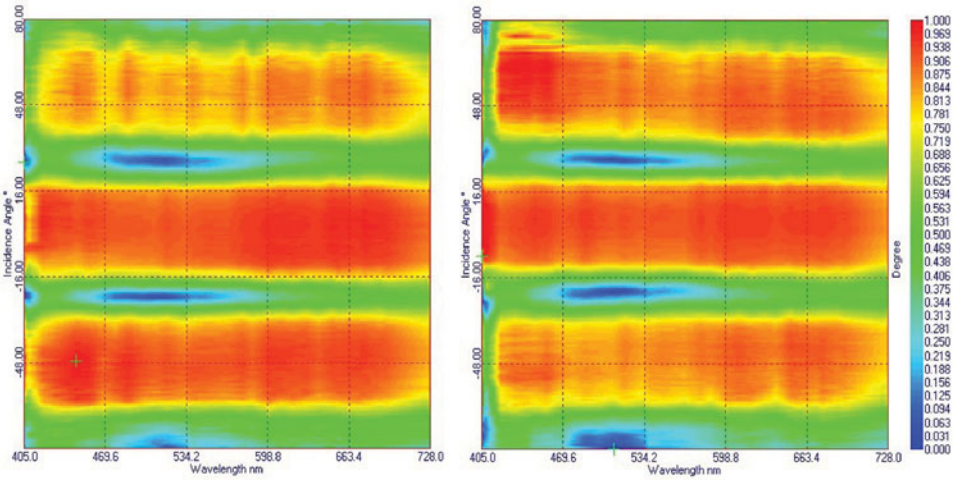

Figure 11. Polarization degree for left eye view and right eye view versus wavelength and incidence angle along vertical azimuth.

dependent on the wavelength as reported in Fig. 12. The polarization state is nearly circular at 530 nm but drop down rapidly in the blue and red regions. This is due to the phase shift behavior in 1/λ of a simple single layer retarder sheet.

Each glass filter is a combination of a retarder plate followed by a polarizer. Using the stokes vector measured by EZContrastMS makes it possible to extrapolate the radiance that should be detected after one or the other circular polarizers for left and right view measurements (cf. Fig. 9a and 10). For each wavelength, the signal seen by the eye of the observer is obtained by the first term of the product of the Stokes vector with the Mueller matrixes of a retarder plate and a polarizer using:

$$\frac{1}{2}R(-\theta)\begin{bmatrix} T & T & 0 & 0 \\ T & T & 0 & 0 \\ 0 & 0 & 0 & 0 \\ 0 & 0 & 0 & 0 \end{bmatrix} * R(\theta) * R(-\alpha) * . \begin{bmatrix} 1 & 0 & 0 & 0 \\ 0 & 1 & 0 & 0 \\ 0 & 0 & \cos\varphi & \sin\varphi \\ 0 & 0 & -\sin\varphi & \cos\varphi \end{bmatrix} * R(\alpha) * \begin{bmatrix} I \\ Q \\ U \\ V \end{bmatrix}$$

Θ and α are the orientations of the polarizer and the retarder plate respectively, φ the phase shift of the retarder plate, T the transmission of the polarizer, and R(θ) the matrix of rotation θ given by:

$$R(\theta) = \begin{bmatrix} 1 & 0\cos & 0 & 0 \\ 0 & 2\theta & \sin 2\theta & 0 \\ 0 & -\sin\ 2\theta & \cos\ 2\theta & 0 \\ 0 & 0 & 0 & 1 \end{bmatrix}$$

In practice we have $\alpha = 0$ and $\theta = 45^\circ$ or $\theta = -45^\circ$ for the two circular polarizers and the signal seen by the left and right eyes of the observer is given by:

$$I_{+45^\circ} = \frac{T}{2}(I + U\cos\varphi + V\sin\varphi) \quad I_{-45^\circ} = \frac{T}{2}(I - U\cos\varphi - V\sin\varphi)$$

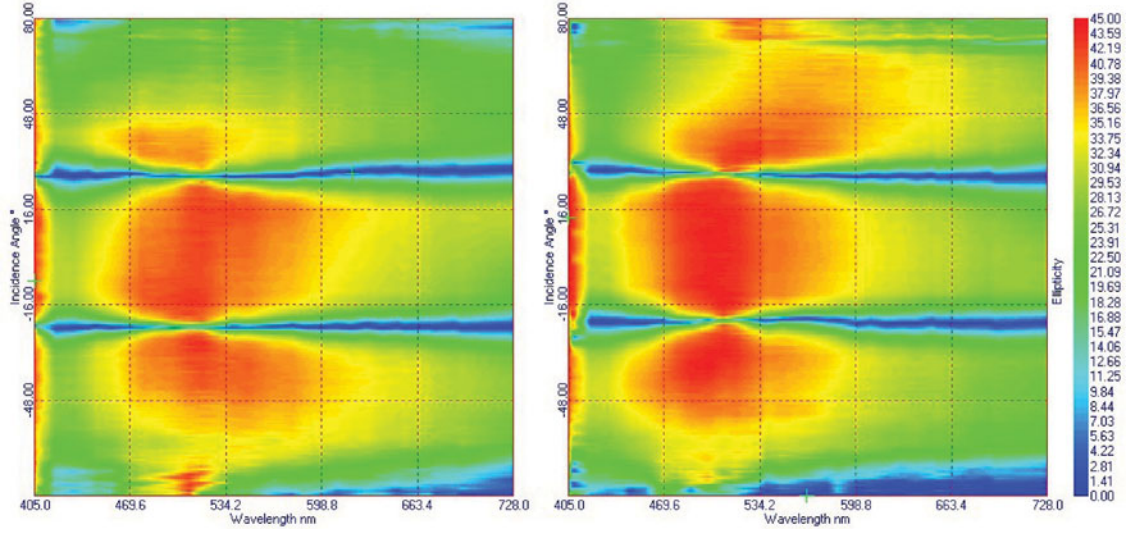

Figure 12. Ellipticity angle for left eye view and right eye view versus wavelength and incidence angle along vertical azimuth.

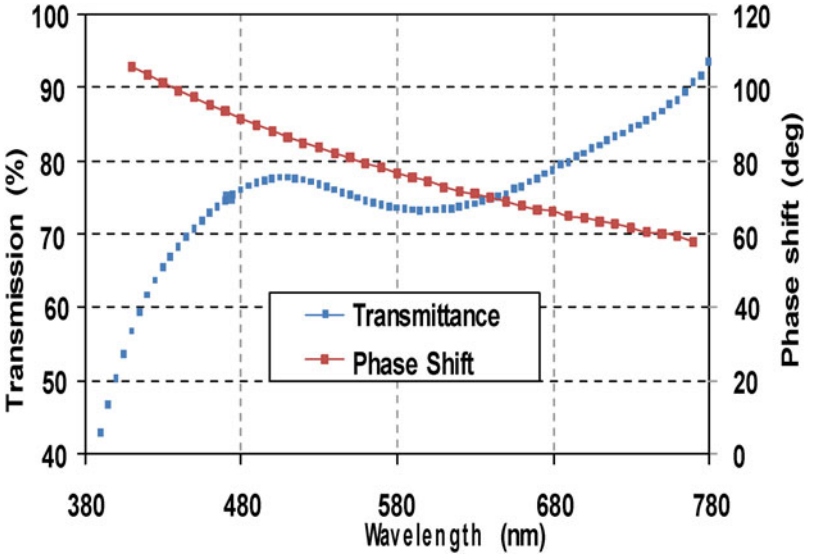

Figure 13. Measured transmittance and phase shift of the polarizer and retarder of glass filters for luminance computation.

To get a more realistic computation we have measured the transmittance of the polarizer and the phase shift of the retarder included inside the glasses using a spectrophotometer and a spectroscopic ellipsometer (cf. Fig. 13). Using these data and the spectral emission measured for each view we have computed the radiance that will be detected after the two glass filters and also the luminance by integrating the radiance with the Y CIE curve. Results for left filter and right view at different wavelengths are reported in Fig. 14. The impact of the non-optimized ellipticity value outside 520nm is particularly clear with the occurrence of crosstalk in the blue and red regions near normal incidence. From the different radiance patterns at the different wavelengths it is then possible to compute the luminance patterns as shown in Fig. 15. These computed luminance patterns can be compared to direct measurements made using luminance viewing angle instrument and additional glass filters located inside the instrument near the diaphragm location (cf. Fig. 1a).

3D Contrast & Crosstalk

Using Fourier optics viewing angle measurement makes it possible to evaluate the light arriving from this display location to an observer located in front of the display. The observer is defined by his coordinates in the XYZ referential. The origin O is always the display center (cf. Fig. 16a). The X axis, Y axis and Z axis define the transverse, sagittal and coronal planes respectively as schematically reported in Fig. 16b. The observer position is supposed to be the center of its two eyes. The inter-pupillar distance is fixed (generally 6.25 cm). For each observer position we can calculate the two couples of polar angles (θ_L, φ_L) and (θ_R, φ_R) using the following formula:

$$\tan\theta = \frac{\sqrt{(y_o - y_e)^2 + (x_o - x_e)^2}}{z_o} \text{ and } \tan\varphi = \frac{y_o - y_e}{x_o - x_e}$$

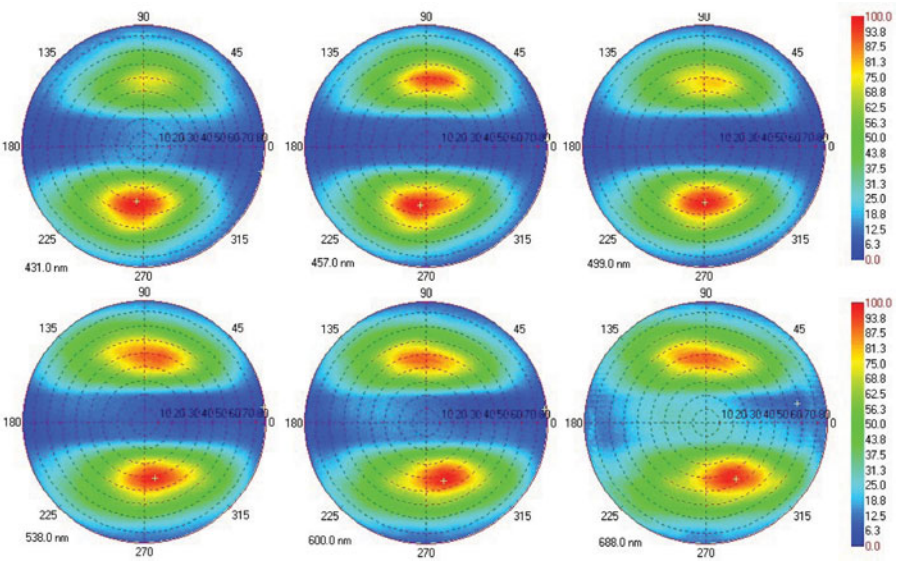

Figure 14. Computed radiance across left filter for right view for different wavelengths.

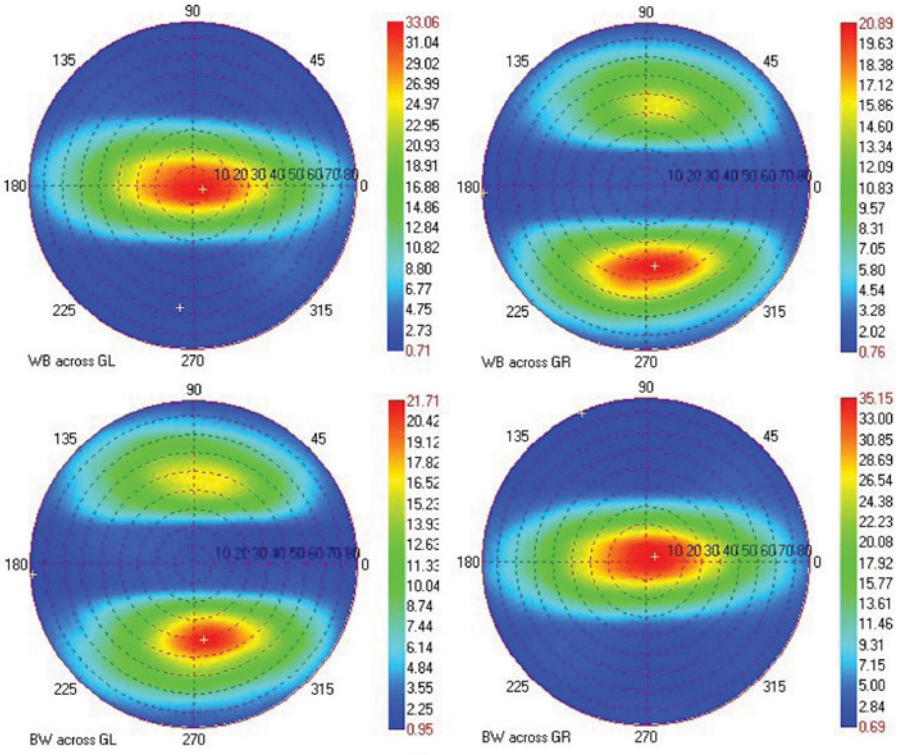

Figure 15. Computed luminance for right and left views across right and left filters.

(x_o, y_o, z_o) are coordinates of the left or the right eye of the observer in XYZ referential and (x_e, y_e, 0) are coordinates of the emissive point of the display in XYZ referential. The orientation of the head of the observer has to be considered while evaluating the polar angle especially at high incidence angles. Calculations have been performed in two limit configurations: either the observer keeps the eyes axis always perpendicular to the display surface or the eyes axis remains perpendicular to the staring direction. Of course both results are similar near normal incidence.

The quality of the 3D display for an observer is directly related to its capacity to clearly display the correct images in his right and left eyes. In case of stereoscopic displays, the two contrasts associated to each eye must be calculated using the two sets of measurements obtained with GL and GR filters using the following equations:

$$C_L = \frac{Y^{GL}_{LWRK}(\theta_L, \varphi_L) - Y^{GL}_{LKRK}(\theta_L, \varphi_L)}{Y^{GL}_{LKRW}(\theta_L, \varphi_L) - Y^{GL}_{LKRK}(\theta_L, \varphi_L)} \qquad C_R = \frac{Y^{GR}_{LKRW}(\theta_R, \varphi_R) - Y^{GR}_{LKRK}(\theta_R, \varphi_R)}{Y^{GL}_{LWRK}(\theta_R, \varphi_R) - Y^{GL}_{LKRK}(\theta_R, \varphi_R)}$$

(θ_R, φ_R) and (θ_L, φ_L) are the right and left eye positions in polar coordinates with regards to the measurement location as mentioned previously. Y_{KLRW} is the luminance for white view on right eye and black view on left eye, Y^{GL}_{LWRK} and Y^{GR}_{LWRK} are the luminances for black view on right eye and white view on left eye using GL and GR filters respectively, Y^{GL}_{RKLK} and Y^{GL}_{RKLK} are the luminance for black view on both eyes. Luminance angular contrasts have been calculated using the luminance patterns computed in Fig. 15. The result for central location is reported in Fig. 17. These diagrams show sharp $+20^\circ$ and 20° widths horizontal bands around normal incidence. The maximum of contrast is around 20 for right eye and 15 for left eye. The contrast is not symmetric and clearly worse on one eye than on the other. The origin of the effect is probably due to fabrication of the phase difference film.

The 3D quality is optimum when the two previous contrasts are maximized simultaneously. It is useful to combine the two monocular contrasts into a so called 3D contrast given by:

$$C^{3D} = \sqrt{C_R(\theta_R, \varphi_R) * C_L(\theta_L, \varphi_L)}$$

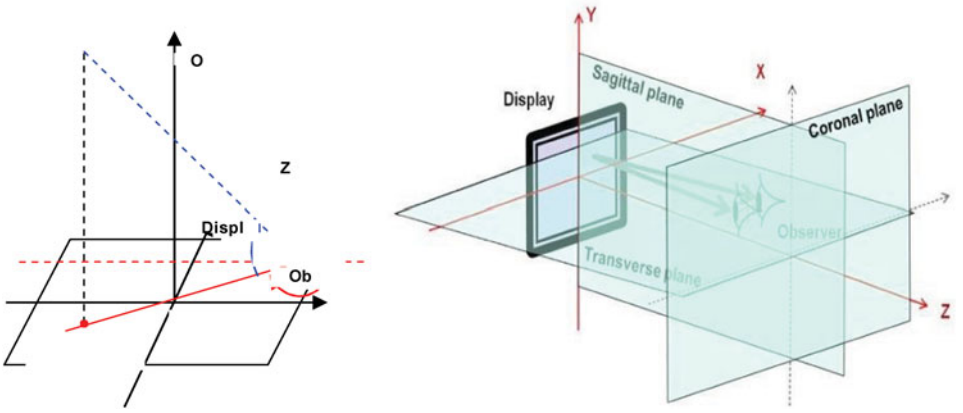

Figure 16. Definition of the system of coordinates (left) and of the different planes for the observer location (right).

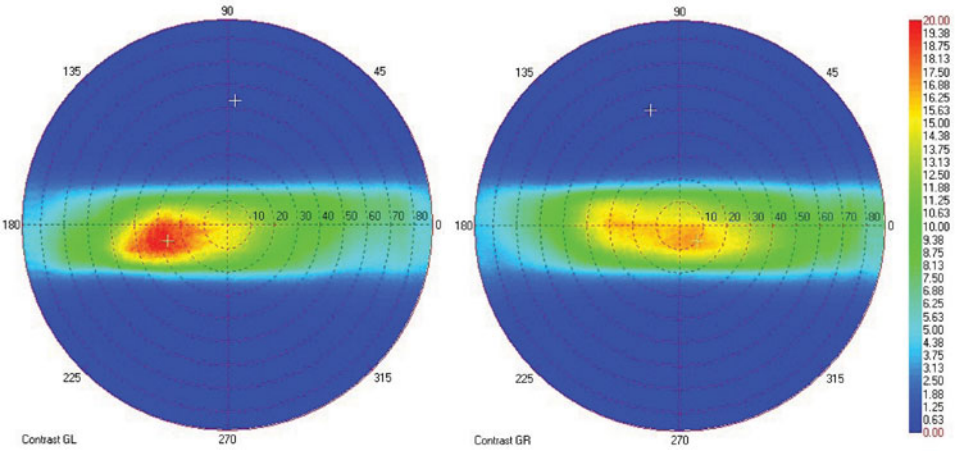

Figure 17. Angular luminance contrast for left and right views at central location.

A product has been chosen instead of a sum because a good 3D quality requires a good contrast simultaneously for left and right eyes. The square maintains the dimension of the quantity as a contrast which can be compared to the standard contrast of displays. These calculations are very similar to those applied to auto-stereoscopic 3D displays but each contrast is obtained separately using the two GL and GR filters [7, 8]. When measurements made at different locations on the display are analyzed simultaneously, the different contrasts for each eye are calculated using previous equations, and the minimum value of these contrasts for the different locations is taken using:

$$C_L = Min_{i=1}^{M} C_L^i \text{ and } \quad C_R = M_{i=1}^{M} C_R^i$$

with M the number of measurement locations. Then the 3D Contrast can be calculated. The maximum of left, right and 3D contrast are used to define Qualified Monocular and Binocular Viewing Spaces (QMVS and QBVS) where the different locations are simultaneously seen with an optimum 3D quality.

Using the angular contrasts, the monocular contrasts and 3D contrast can be calculated for a given volume in front of the display. We have made different computation in a volume of 2000 × 2000 × 4000 mm in front of the display. 3D contrast computation along the sagittal plane for central measurement location and 3 vertical measurement locations are

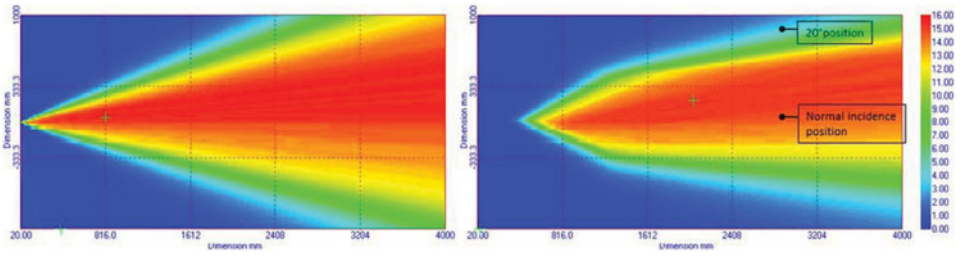

Figure 18. 3D contrast computed for the central location measurement (top) and the three vertical locations (bottom) along the sagittal plane: the location of the imaging instrument is also reported.

reported in Fig. 18. The qualified binocular viewing space is precisely defined by these computations.

Local Defects with Polarization Imaging

The previous analysis is based on a limited number of local measurements. Local defects on the display surface cannot be detected easily. In order to measure the possible local variations, we have located the UMaster imaging system at two positions in front of the display (cf. Fig. 18). The first position is on axis at a distance of 3 meters in the middle of the QBVS. The other position is tilted of around 20° along the top at the limits of the QBVS. The polarization state of the light emitted by the entire surface of the display at 550nm for left view on and right view off are reported in Fig. 19 for the two configurations. In agreement with the viewing angle measurement results summarized above, we measure a polarization degree near 1 for the entire display surface view on axis. The ellipticity is also closed to 45° near the optimized value. Nevertheless, the tilted configuration provides a polarization degree and an ellipticity which are correct only for the bottom of the display. All the top part of the display emits light that is not completely polarized. In addition this

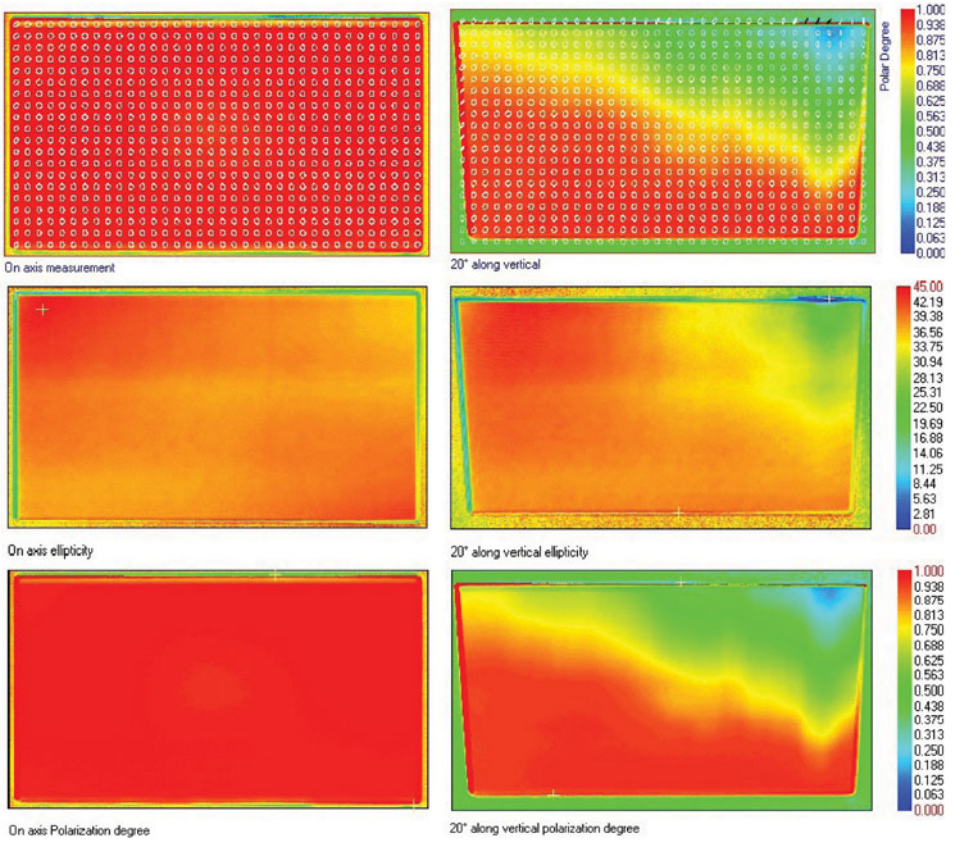

Figure 19. Polarization state of the light (top), ellipticity (center) and polarization degree (bottom) measured on the full surface of the passive glass 3D TV for left view on with the imaging system on axis (left) and at 20° along the vertical (right).

effect is not symmetric on each side of the display. The top right side is much more affected than the left side. The origin of this effect is certainly related to a small misalignment of the top phase shift film apply on this type of display. In other cases, local "polarization MURA" defects have been detected [13].

Conclusions

We have shown that the measurement of the polarization state of the light is a powerful tool for the characterization of displays and their components. Different instruments for viewing angle and imaging measurements have been developed by ELDIM for these particular applications. For the display components (films, polarizers, wave plates . . .) one of the main interest of the Fourier optics solution compared to standard polarimetry, in addition to the measurement speed is the capacity to measure the film in a "true" illumination environment comparable to the final use in LCDs. Indeed, measurement results made with a pseudo Lambertian lamp integrate the diffused light and offer more realistic characteristics than simple collimated beam measurements. Collimated beam measurement can nevertheless be made with the same instrument and the full diffused behavior (polarized BTDF) can be estimated very rapidly. For LCD modules, the polarization modulation of the liquid crystal cell can be precisely measured at each grey level. Precise characterization of the light emitted in OFF state is also useful to understand the key parameters driving the performances of such displays. In the particular case of the passive glass 3D displays the polarization analysis is extremely powerful to understand and quantify the impact of the different imperfections on the standard and stereoscopic properties. We have shown that the present commercial TVs suffer from different drawbacks: the polarization is modulated vertically and the useful volume in front of the display is not maximized. The top phase shift film should be included closed to the crystal cell to avoid such problems. The ellipticity is circular only in the green but becomes elliptic in the blue and the red inducing colors shifts for the observer in addition to the crosstalk. This is due to the spectral dependence of the top phase shift film. Much better properties could be obtained with achromatic phase shift films. The polarization states of the two views are not completely symmetric, an effect that is probably related to the fabrication process of the phase shift film itself. Auto-stereoscopic 3D displays can also exhibit complex polarization behavior due to the impact of the micro-lenses especially when liquid crystal lenses are used [15]. The polarization analysis can help understanding the origin of the imperfections of such displays where the light emission must be controlled very accurately.

References

[1] McMurry, J. (1995). *Organic Chemistry*, 3rd ed., Brooks/Cole, Pacific Grove, CA.
[2] Baba, J., Chung, J., DeLaughter, A., Cameron, B., & Coté, G. (2002). *J. Biomedical Optics*, *7*(3), 341.
[3] Boher, P., Bignon, T., & Leroux, T. (2007). "Angle of View Polarization Characterization of Liquid Crystal Displays and Their Components," *Journal of Information Display*, Vol. 8, N. 4, 10–14.
[4] Boher, P., Leroux, T., Bignon, T., & Glinel, D. (2008). "New multispectral Fourier optics viewing angle instrument for full characterization of LCDs and their components," SID, Los Angeles, CA.
[5] Boher, P. (2008). "*Checks of polarization shed light on LCD characteristics*," Display Devices, Spring.

[6] Boher, P., Bignon, T., Glinel, D., & Leroux, T. (2008). "Viewing angle and spectral characterization of LCDs and their components," IDW, Niigata, Japan.
[7] Boher, P., Leroux, T., Bignon, T., & Collomb-Patton, V. (2010). "*Multispectral polarization viewing angle analysis of circular polarized stereoscopic 3D displays*," SPIE, San Jose, CA, January18–21.
[8] Boher, P., Leroux, T., Collomb-Patton, V., & Bignon, T. (2009). "Polarized based stereoscopic 3D display characterization using Fourier optics instrument & computation in the observer space," IDW, Miyazaki, Japan, December 9–11, 3D4-3.
[9] Boher, P., Leroux, T., & Glinel, D. (2009). "Polarization imaging for characterization of LCDs and their components," Eurodisplay, Roma, Italy, September.
[10] Boher, P., Leroux, T., & Collomb-Patton, V. (2010). "*Imaging polarization for characterization of polarization based stereoscopic 3D displays*," Electronic Imaging, SPIE, San Jose, CA, January 18–21.
[11] Boher, P., Leroux, T., Collomb-Patton, V., Bignon, T., & Ginel, D. (2010). "Viewing Angle and Imaging Polarization Analysis of Polarization Based Stereoscopic 3D Displays," SID, May, Seattle, WA.
[12] Boher, P., Leroux, T., Collomb-Patton, V., Bignon, T., & Ginel, D. (2010). "A common approach to characterizing auto-stereoscopic and polarization-based 3-D displays," *Journal of the SID*, *18/4*, 293.
[13] Boher, P., Leroux, T., & Bignon, T. (2011). "Crosstalk homogeneity of passive glass 3D displays," IMID, Seoul, Korea, October 11–15, 34-2
[14] Boher, P., Leroux, T., Bignon, T., & Blanc, P. (2011). "Passive glass 3D display crosstalk characterization," IDW, Nagoya, Japan, December 7–9.
[15] Boher, P., Leroux, T., Bignon, T., & Collomb-Patton, V. (2012). "New applications of viewing angle polarization analysis for characterization of displays," IDW, Kyoto, Japan, December 4–7.
[16] Leroux, T. (1993). "Fast contrast vs viewing angle measurements of LCDs," Eurodisplay, Strasbourg, 447.
[17] Berry, H., Gabrielse, G., & Livingston, A. (1977). "Measurement of the Stokes parameters of light," *Appl. Optics*, Vol. *16*, N. 12, 3200.
[18] Tyo, J., Goldstein, D., Chenault, D., & Shaw, J. (2006). "Review of passive imaging polarimetry for remote sensing applications," *Appl. Optics*, Vol. 45, N. 22, 5453.
[19] Tang, S. T., & Kwok, H. S. (2001). "3 × 3 matrix for unitary optical systems," *J. Opt. Soc. Am., A*, Vol. 18, N. 9, 2138.